

Implementation of a quantum algorithm to solve the Bernstein-Vazirani parity problem without entanglement on an ensemble quantum computer

Jiangfeng Du,* Mingjun Shi, Xianyi Zhou, Yangmei Fan, Bangjiao Ye, and Rongdian Han
 Laboratory of Quantum Communication and Quantum Computation, University of Science and Technology of China,
 Hefei 230026, People's Republic of China

and Department of Modern Physics, University of Science and Technology of China, Hefei 230027, People's Republic of China

Jihui Wu

Laboratory of Structure Biology, University of Science and Technology of China, Hefei 230026, People's Republic of China
 (Received 19 December 2000; revised manuscript received 30 May 2001; published 11 September 2001)

Bernstein and Vazirani have given the first quantum algorithm to solve the parity problem in which a strong violation of the classical information theoretic bound comes about. In this paper we refine this algorithm with fewer resources and implement a two-qubit algorithm in a single query on an ensemble quantum computer.

DOI: 10.1103/PhysRevA.64.042306

PACS number(s): 03.67.Lx

Associated with the model of a quantum computer [1,2], a variety of quantum algorithms have been proposed [3–7]. In the theoretical view, these algorithms have relevance to the entanglement phenomena, the peculiar quantum property identified by Erwin Schrödinger [8], which is invoked as the mechanism for the speedup of quantum computing over their classical counterpart [9]. Until recently these algorithms were only of theoretical interest, as it proved extremely difficult to build a quantum computer. In the last few years, however, there has been substantial progress based on nuclear magnetic resonance (NMR) [10]. Up to now some simple quantum algorithms have been realized step by step on a NMR quantum computer, including Deutsch's algorithm [11–17], Grover's algorithm [18–22], and ordering find's algorithm [23]. However, a sharp criticism has been proposed by Braunstein *et al.* that NMR experiments have not actually realized quantum algorithm because at each step the state of the system can be described as a probabilistic ensemble of unentangled quantum states [24]. On the other hand, some scientists believe that for a specific quantum algorithm the power of a quantum computer derives from quantum superposition and parallelism, other than entanglement [25–28].

The problem we considered in this paper is the parity problem about a database A that contains an arbitrary n -bit string a . The answer to queries represented by n -bit string x to the database is the parity of the bits common to x and a given by $(a,x) = a \cdot x$. Note that the problem is to determine a in its entirety, not to merely determine the parity of a . The classical determination of an n -bit string a requires at least n query operations (since n -bit string a contains n bits of information and each classical evaluation of query operation yields a single bit of information). Bernstein and Vazirani have given the first quantum algorithm in which n -bit string a can be determined in only two queries to the database [6]. But by preparing the output one-bit register in an initial superposition $(1/\sqrt{2})(|0\rangle - |1\rangle)$, the algorithm can be simplified to comprise a single query [29]. Terhal and Smolin rediscovered this algorithm, which was underappreciated, to

solve binary problems and coin-weighing problems effectively [30].

In this paper, based on Bernstein-Vazirani's parity problem [6], we propose a scheme to solve this problem by using less physics resource than the previous algorithm [28,29], but without loss of effectivity. Further, we demonstrate this algorithm on a two-qubit NMR quantum computer.

Bernstein and Vazirani's parity problem can be described as a function $f: \{0,1\}^n \rightarrow \{0,1\}$, which is of the form $f_a(x) = a \cdot x \equiv (\sum_{i=1}^n a_i x_i) \pmod{2}$, where n -bit strings a , $x \in \{0,1\}^n$, a_i and x_i are the i th bits of a and x , and $a \cdot x$ denotes the bitwise AND (or mod 2 scalar product), $a \cdot x \equiv (a_1 \wedge x_1) \oplus (a_2 \wedge x_2) \oplus \dots \oplus (a_n \wedge x_n)$. The answer is to find the n -bit string a . The previous quantum algorithm [28,29] solved this problem theoretically by a pair of registers (x, b) , where $x \in \{0,1\}^n$, $b \in \{0,1\}$. The quantum network to implement the algorithm is shown in Fig. 1, the $n+1$ qubits register (x, b) start in the state $|x\rangle|b\rangle = (|0\rangle)^n (1/\sqrt{2})(|0\rangle - |1\rangle)$. The function $f_a(x) = a \cdot x$ is designed within a unitary operator U_f which denotes the transform

$$U_f |x\rangle|b\rangle \rightarrow |x\rangle|y \oplus f(x)\rangle \equiv |x\rangle|b \oplus (a \cdot x \pmod{2})\rangle.$$

The Hadamard gate H denotes the transform

$$|0\rangle \rightarrow \frac{1}{\sqrt{2}}(|0\rangle + |1\rangle),$$

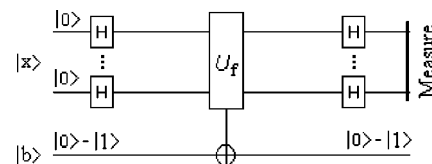


FIG. 1. A (schematic) quantum circuit implementing Bernstein-Vazirani's algorithm in a single query. The upper n line corresponds to n qubits of register X , while the lower line corresponds to one qubit of register b .

*Email address: djf@ustc.edu.cn

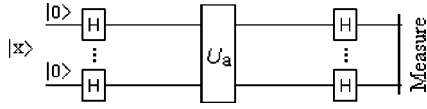


FIG. 2. The (schematic) refined version of the quantum circuit shown in Fig. 1; note that one-qubit register b is removed by changing the unitary operator.

$$|1\rangle \rightarrow \frac{1}{\sqrt{2}}(|0\rangle - |1\rangle),$$

$$H = \frac{1}{\sqrt{2}} \begin{pmatrix} 1 & 1 \\ 1 & -1 \end{pmatrix}.$$

If we apply n Hadamard gates $H^{(n)} = H \otimes H \otimes \dots \otimes H$ parallel to an n qubit, then the n -qubit state transforms as

$$H^{(n)}: |x\rangle \rightarrow \frac{1}{\sqrt{2^n}} \sum_{y=0}^{2^n-1} (-1)^{x \cdot y} |y\rangle.$$

Therefore, acting on the input $(|0\rangle)^n (1/\sqrt{2})(|0\rangle - |1\rangle)$, with $f_a(x) = a \cdot x$ and $(1/2^n) \sum_{y=0}^{2^n-1} (-1)^{a \cdot x + x \cdot y} = \delta_{ay}$, we can evaluate the state of the input register as

$$\begin{aligned} (|0\rangle)^n |1\rangle &\xrightarrow{H^{(n+1)}} \frac{1}{\sqrt{2^n}} \sum_{x=0}^{2^n-1} |x\rangle \otimes \frac{|0\rangle - |1\rangle}{\sqrt{2}} \\ &\xrightarrow{U_f} \frac{1}{\sqrt{2^n}} \sum_{x=0}^{2^n-1} (-1)^{f_a(x)} |x\rangle \otimes \frac{|0\rangle - |1\rangle}{\sqrt{2}} \\ &\xrightarrow{H^{(n)}} \frac{1}{\sqrt{2^n}} \sum_{x=0}^{2^n-1} \sum_{y=0}^{2^n-1} (-1)^{a \cdot x + x \cdot y} |y\rangle \otimes \frac{|0\rangle - |1\rangle}{\sqrt{2}} \\ &\equiv |a\rangle \otimes \frac{|0\rangle - |1\rangle}{\sqrt{2}}. \end{aligned}$$

It is obvious that one could execute the quantum network once and measure the n -qubit input register, finding the n -bit string a in the function $f_a(x) = a \cdot x \equiv (\sum_{i=1}^n a_i x_i) \bmod 2$ with probability 1.

Our refined version of the Bernstein-Vazirani algorithm uses n qubits rather than $n+1$ qubits, to find n bits string a . A quantum circuit for this refined quantum algorithm is shown in Fig. 2. To compare with the original algorithm shown in Fig. 1, the one-qubit work register b is removed because it is redundant in the sense that its state does not change. To do so, the binary function $f_a(x) = a \cdot x$ encoded in a $n+1$ qubits unitary transformation U_f was changed into the n -qubit propagator U_a such that

$$U_a |x\rangle \rightarrow (-1)^{f_a(x)} |x\rangle,$$

and the unitary transformation U_a can be decomposed as direct products of single-qubit operators

$$U_a = U^1 \otimes U^2 \otimes \dots \otimes U^i \otimes \dots \otimes U^{n-1} \otimes U^n,$$

$$U^i = \begin{cases} I, & a_i = 0 \\ \sigma_z, & a_i = 1 \end{cases}, \quad I = \begin{pmatrix} 1 & 0 \\ 0 & 1 \end{pmatrix}, \quad \sigma_z = \begin{pmatrix} 1 & 0 \\ 0 & -1 \end{pmatrix}.$$

The first Hadamard gate $H^{(n)} = H \otimes H \otimes \dots \otimes H$ takes $|\psi_0\rangle = (|0\rangle)^n$ to $|\psi_1\rangle = (1/\sqrt{2^n}) \sum_{x=0}^{2^n-1} |x\rangle$. After the unitary transformation U_a responds to this quantum query, the state is $|\psi_2\rangle = (1/\sqrt{2^n}) \sum_{x=0}^{2^n-1} (-1)^{f_a(x)} |x\rangle = (1/\sqrt{2^n}) \sum_{x=0}^{2^n-1} (-1)^{a \cdot x} |x\rangle$. The final Hadamard gate $H^{(n)}$ outputs $|\psi_3\rangle = (1/\sqrt{2^n}) \sum_{x=0}^{2^n-1} \sum_{y=0}^{2^n-1} (-1)^{a \cdot x + x \cdot y} |y\rangle = |a\rangle$. Whereupon measuring the whole n -qubits register identifies a with probability 1 (the output states for different a 's are orthogonal).

Quantum entanglement and quantum interference are usually thought to be the key gradient in a quantum algorithm and the reason why the quantum algorithm exceeds a classical algorithm. But in the above refined quantum algorithm, there is no entanglement in it. The initial state is $|\psi_0\rangle = (|0\rangle)^n$, which is obviously separable. After the Hadamard transformation, the state is $|\psi_1\rangle = (1/\sqrt{2^n})(|0\rangle + |1\rangle) \otimes (|0\rangle + |1\rangle) \otimes \dots \otimes (|0\rangle + |1\rangle)$. Performed by query operations U_a , the state becomes $|\psi_2\rangle = (1/\sqrt{2^n})(|0\rangle + e^{i\pi a_0}|1\rangle) \otimes (|0\rangle + e^{i\pi a_1}|1\rangle) \otimes \dots \otimes (|0\rangle + e^{i\pi a_n}|1\rangle)$. And the state after the second Hadamard transformation is the output state $|\psi_3\rangle = |a_0\rangle |a_1\rangle \dots |a_n\rangle$. In the whole procedure, the state is a tensor product of the states of the individual qubits, so it is unentangled. And because the operators in the algorithm ($H^{(n)}$, U_a , and $H^{(n)}$) are also tensor products of the individual local operators on these qubits; $H^{(n)} = H \otimes H \otimes \dots \otimes H$, $U_a = U^1 \otimes U^2 \otimes \dots \otimes U^i \otimes \dots \otimes U^{n-1} \otimes U^n$. Such a unitary transformation cannot change the entanglement of a state.

Experimentally, this quantum algorithm without entanglement was implemented using the nuclear spins of the two hydrogen atoms in a deuterated cytosine molecule. $|0\rangle(|1\rangle)$ describes the spin state aligned with (against) an externally applied, strong static magnetic field B_0 in the \hat{z} direction. The reduced Hamiltonian for this two-spin system is to an excellent approximation given by

$$H = \omega_A I_z^A + \omega_B I_z^B + 2\pi J_z^A I_z^B,$$

where the first two terms describe the free precession of spins A and B of two hydrogen atoms about B_0 with frequencies $\omega_A/2\pi \approx \omega_B/2\pi \approx 500$ MHz, and the chemical shift $|\omega_A/2\pi - \omega_B/2\pi| = 765$ Hz enables us to address each spin (acting as a qubit) individually. I_z^A is the angular momentum operator in the $+\hat{z}$ direction for A . The third term describes a scalar spin-spin coupling of the two spins of $J \approx 7.17$ Hz. As we know, pulsed radio-frequency (rf) electromagnetic fields, oriented in the \hat{x} - \hat{y} plane perpendicular to the static magnetic field B_0 , selectively address either A or B by oscillating at frequency ω_A and ω_B . For example, an rf pulse along \hat{y} rotates a spin about that axis by an angle θ proportional to $\theta \approx tP$, the product of the pulse duration t and pulse

power P . In this paper we shall let $R_y^A(\theta)$ denote θ rotations that act on spin A about \hat{y} , and $R_x^{AB}(\theta)$ denotes θ rotations that act on spin A and B about \hat{x} simultaneously, and so forth; superscripts will identify which spin the operation acts upon and subscripts denote which axis an rf pulse rotates a spin about.

Experiments are conducted at room temperature and pressure on a Bruker Avance DMX-500 spectrometer at the Laboratory of Structure Biology, University of Science and Technology of China. A quantum circuit for implementing this algorithm on a two-qubit NMR quantum computer is shown in Fig. 2 with $n=2$. In our experiment, pairs of Hadmard gates were replaced by a NMR pseudo-Hadamard gate h (a 90_y rotation) and its inverse h^{-1} [31]. An input pseudopure state $\psi_0=|00\rangle$ was generated using the approach of Cory *et al.* [32,33]. This is implemented as $R_x^B(\pi/3) - G_z - R_x^A(\pi/4) - \tau - R_y^A(-\pi/3) - G_z$, to be read from left to right, where G_z is the pulsed field gradient along the \hat{z} axis to annihilate all transverse magnetizations, dashes are for readability only, and τ represents a time interval of $1/(2J) \approx 69.735$ ms.

The pair of pseudo-Hadamard gates h and h^{-1} could be easily implemented by two hard pulses denoted as $R_{-y}^{AB}(\pi/2)$ and $R_y^{AB}(\pi/2)$; the typical pulse lengths were 10–20 μ s. All unitary transformation U_a corresponding to the query of four possible two-bit string $a=\{00,01,10,11\}$ in the function $f_a(x)=a \cdot x$ could be denoted as $U_{00}=I^A \otimes I^B$, $U_{01}=I^A \otimes \sigma_z^B$, $U_{10}=\sigma_z^A \otimes I^B$, $U_{11}=\sigma_z^A \otimes \sigma_z^B$. The U_{00} transformation corresponds to the unity operation or “do nothing.” U_{01} and U_{10} transforms are separately achieved by applying the $R_z^B(\pi)$ rotation selectively on the second qubit B and the $R_z^A(\pi)$ rotation on the first qubit A . The selective z pulse was implemented by the time evaluation under the Hamiltonian of Eq. (7) with refocusing π pulses applied at suitable times during the evolution period. Since the refocusing π pulse has the effect of time reversal, it can be used to make one term in the Hamiltonian evolve while the other terms “freeze” [34,35]. In our experiment, we extended these method to realize the selective pulses $R_z^A(\pi)$ and $R_z^B(\pi)$ separately as

$$\tau_1/4 - R_x^B(\pi) - \tau_1/2 - R_{-x}^B(\pi) - \tau_1/4,$$

$$\tau_2/4 - R_x^A(\pi) - \tau_2/2 - R_{-x}^A(\pi) - \tau_2/4,$$

where $\tau_1=\tau_2=1.3$ ms and the axes of successive π pulses were chosen in the way to cancel imperfections of selective pulses. U_{11} corresponds to a π rotation $R_z^{AB}(\pi)$ about the axis \hat{z} of both qubits, up to a global phase factor. Global phase changes are not detectable in NMR and are hence ignored for the purpose of experiment. This nonselectively \hat{z} rotation was implemented using a composite-pulse sandwich as a set of \hat{x} and \hat{y} axes $R_{-y}^{AB}(\pi/2) - R_x^{AB}(\pi) - R_y^{AB}(\pi/2)$.

The prediction is that the algorithm will put the spins in the eigenstates $|a\rangle=|ij\rangle$ which can be expressed similarly as

$$|ij\rangle\langle ij| = \frac{1}{2} [(-1)^i I_x^A + (-1)^j I_z^B + (-1)^{i \oplus j} 2 I_x^A I_z^B].$$

With the application of a selective readout pulse $R_y^A(\pi/2)$, it gives

$$\frac{1}{2} [(-1)^i I_x^A + (-1)^j I_z^B + (-1)^{i \oplus j} 2 I_x^A I_z^B]$$

and the observable signal is proportional to

$$(-1)^i [I_x^A + (-1)^j 2 I_x^A I_z^B].$$

Thus only one of the two lines in the A spin doublet will be observed; which one of the two peaks will be observed depends on j , the state of spin B , while the phase of the signal depends on i , the state of spin A . Therefore, both the phase of the peak in the spectrum and the position of the peak in the spectrum of each spin could be used to determine the eigenstates $|a\rangle=\{|00\rangle,|01\rangle,|10\rangle,|11\rangle\}$ before the readout selective pulse. Figure 3 shows the result spectra of the algorithm. It is clear that our implementation of the quantum algorithm by using a single query leaves the computer in the final state $|a\rangle$, much as expected. However, there are visible imperfections in the result spectra. To show how good the algorithm has been implemented, we also characterized the entire density matrix $\rho=\rho_\Delta + \text{Tr}(\rho)/4$ (Fig. 4) describing the pseudopure input state and the four final two-qubit states, which were made by using so-called quantum state tomography [6]. The procedure was to apply a sequence of rf pulses, measure the resulting induction signal, Fourier transform to get the spectra, and integrate to get the areas of the resonance peaks. By applying nine different pulse sequences (no rotation, rotation about \hat{x} , and about \hat{y} for each of the two spins), the elements in the density matrix were sampled, allowing a least-squares procedure to recover the density matrix from the data. In Fig. 4 we show the fidelities of the pseudopure state ρ_{in} and the result states ρ_a compared to the ideal eigenstate $|a\rangle$, determined by the equation $F = \langle a | \rho_a | a \rangle$.

The fidelities of the result states ρ_a vary from 93% to 95%. The errors of the result states ρ_a are primarily due to the imperfection of the prepared pseudopure state ρ_{in} with a fidelity of 96%. The other errors are primarily due to the imperfection of the selective pulses used in computation and readout procedure, off-resonance effects of pulses, and other smaller errors coming from the readout procedure (in order of importance). First, the important source of errors in the experiments is the rf field inhomogeneity and imperfection of the selective pulses in our two-qubit homonuclear spin system. In practice it is difficult for a selective pulse to achieve the desired effect at one spin while leaving the other entirely unaffected. In order to achieve a good selectivity the length of the selective pulse is about 5.23 ms in our experiments while in this period the evolution of the other spin induces errors which are difficult to reduce. We notice that such errors (shown in Figs. 3 and 4) are more severe in the case of ρ_{01} and ρ_{10} , in which cases there are U_{01} and U_{10} unitary operations where the selective pulses are used, and less severe in the case of ρ_{00} and ρ_{11} , in which cases there are U_{00} and U_{11} unitary operations where no selective pulses are used. Second, the contribution to errors is the off-

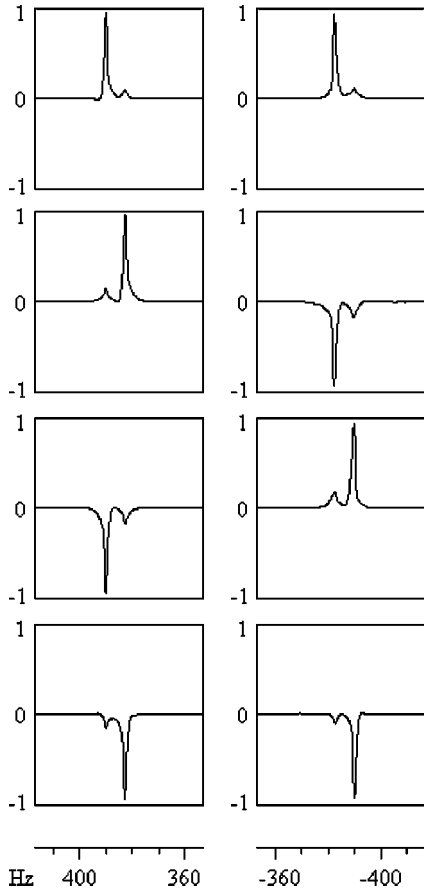


FIG. 3. Proton spectrum after completion of the quantum algorithm and a selective readout pulse, with a pseudopure input state $|00\rangle$. The left-hand pair of signals corresponds to the proton spectra of spin A obtained by the selective readout pulse $R_y^A(\pi/2)$, while the pair at the right hand corresponds to the proton spectra of spin B obtained by the selective readout pulse $R_y^B(\pi/2)$. Each proton spectrum is the Fourier-transformed time varying voltage $V(t)$, induced in the pickup coil by the precession of this spin about $-B_0$ after a selective readout pulse. Only the real parts of the spectra are shown, with NMR peaks at $(\omega_A \pm \pi J_B)/2\pi$ and $(\omega_B \pm \pi J_A)/2\pi$ (shown in Hz relative to the center of the proton spectrum), and the vertical scale is in the same arbitrary units. The phase and the position of the peaks clearly indicate the two-bit string a equal to 00, 01, 10, and 11 (from top to bottom), see text.

resonance effects [10]. In our experiment, the applied rf field is not perfectly resonant with the NMR transitions, but instead is applied a small distance $[\pm(\omega_A - \omega_B)/4\pi = \pm 382.5 \text{ Hz}]$ away. Thus the effect of the field (in the rotating frame) is not simply to cause a rotation around itself, but rather to cause a rotation around a tilted axis. The other smaller contribution to errors may come from the readout procedure, such as the numerical errors in the data analysis. Taking these errors into consideration, we can say the results are remarkably good, as it is still easy to determine the result state of the algorithm because our computer is small and the pulse sequences that run on it are short. The longest computation in our experiment took less than 12 ms., which is well within the decoherence time $T_2 \approx 3 \text{ s}$, hence all the spectra in Fig. 3 have similar amplitudes.

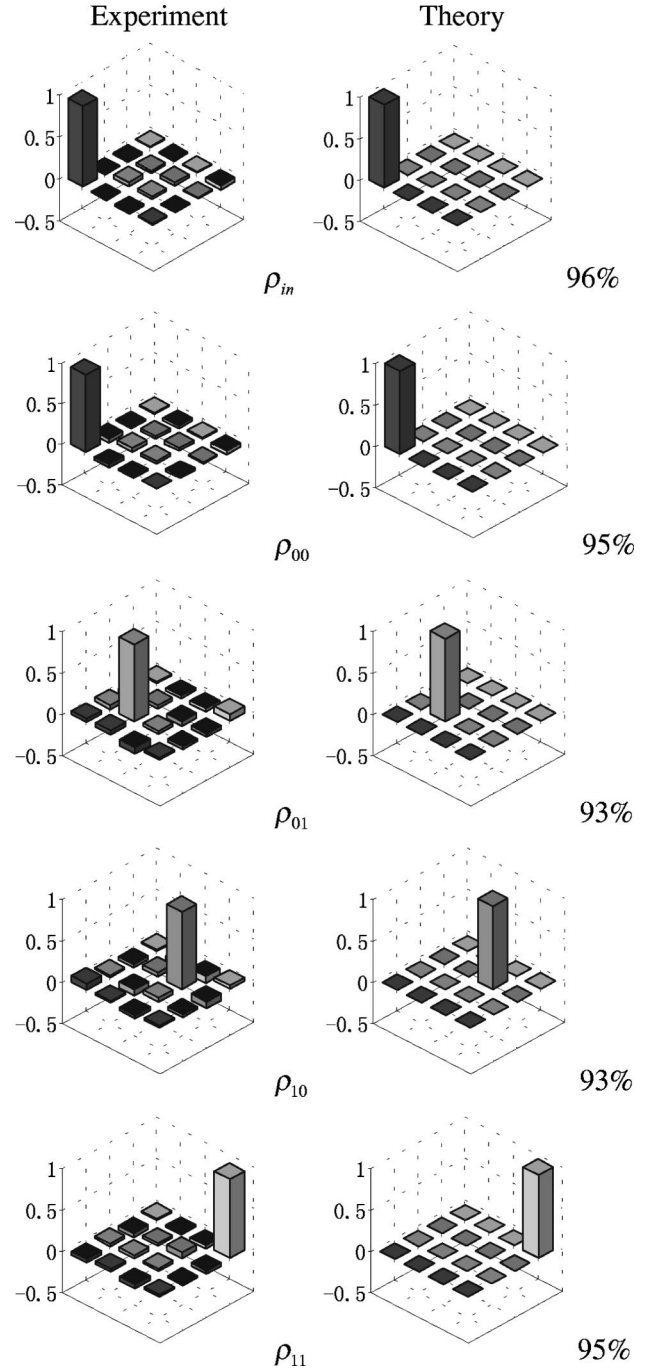


FIG. 4. Experimentally measured and theoretically expected density matrices of the pseudopure input state ρ_{in} and the four output two-qubit states ρ_a after completion of the quantum algorithm. The diagonal elements represent the normalized populations of the states $|00\rangle$, $|01\rangle$, $|10\rangle$, and $|11\rangle$ (from left to right). The off-diagonal elements represent coherence between different states. The magnitudes are shown with the sign of the real component; all the imaginary components are small. In the experiments, the normalized pure-state population (ideally equal to 1) varied from 0.975 to 1.005. The other density matrix elements (ideally 0) are smaller than 0.08 in magnitude. The fidelities of the pseudopure state ρ_{in} and the result states ρ_a compared to the ideal eigenstate $|a\rangle$ determined by the equation $F = \langle a | \rho_a | a \rangle$ varied from 93% to 96%, which are shown in the right-hand side of figure.

To summarize, we have presented a refined version of Bernstein and Vazirani's quantum algorithm with fewer resources and implemented this algorithm in a single query on an ensemble quantum computer. This algorithm, which violates the classical information theoretic bound [30] and a clear separation between the quantum and classical difficulty of the problem [6], reduces the number of queries all the way from n to 1. It is obvious that in this algorithm there is neither an entangle state nor an entangle transformation, only the concept of coherent superposition is exploited to prepare "in parallel" an input state which is a superposition of all possible classical inputs. Our algorithm and its experimental

realization demonstrate that the superposition principle brings about a more effective and concise procedure even if the entanglement phenomena do not occur. As we all know, some quantum algorithms have relevance with entanglement [3,7], but some others do not [25–28], so it is meaningful to know the role of entanglement in quantum algorithms, i.e., the relationship between the entanglement and the complexity of the algorithm.

This project was supported by the National Nature Science Foundation of China (Grants No. 10075041 and No. 10075044) and the Science Foundation of USTC for young scientists.

-
- [1] R. P. Feynman, *Int. J. Theor. Phys.* **21**, 467 (1982).
 [2] D. Deutsch, *Proc. R. Soc. London, Ser. A* **400**, 97 (1985).
 [3] P. W. Shor, in *Proceedings of the 35th Annual Symposium on Foundations of Computer Science*, edited by S. Goldwasser (IEEE Computer Society Press, Los Alamitos, CA, 1994), p. 124.
 [4] D. Deutsch and R. Josza, *Proc. R. Soc. London, Ser. A* **439**, 553 (1992).
 [5] L. K. Grover, *Phys. Rev. Lett.* **79**, 325 (1997).
 [6] E. Bernstein and U. Vazirani, *SIAM J. Comput.* **26**, 1411 (1997).
 [7] D. R. Simon, in *Proceedings of the 35th Symposium on Foundation of Computer Science* (Ref. [3]), p. 116.
 [8] E. Schrödinger, *Naturwissenschaften* **23**, 807 (1935); **23**, 823 (1935); **23**, 844 (1935).
 [9] A. K. Ekert and R. Josza, *Rev. Mod. Phys.* **68**, 733 (1996); A. K. Ekert and R. Josza, *Philos. Trans. R. Soc. London, Ser. A* **356**, 1769 (1998).
 [10] R. R. Ernst, G. Bodenhausen, and A. Wokaun, *Principles of Nuclear Magnetic Resonance in One and Two Dimensions* (Clarendon, Oxford, 1987); D. G. Cory, A. F. Fahmy, and T. F. Havel, *Proc. Natl. Acad. Sci. U.S.A.* **94**, 1634 (1997); N. A. Gershenfeld and I. L. Chuang, *Science* **275**, 350 (1997).
 [11] I. L. Chuang, L. M. K. Vandersypen, X. Zhou, D. W. Leung, and S. Lloyd, *Nature (London)* **393**, 143 (1998).
 [12] J. A. Jones and M. Mosca, *J. Chem. Phys.* **109**, 1648 (1998).
 [13] K. Dorai, Arvind, and A. Kumar, *Phys. Rev. A* **61**, 042306 (2000).
 [14] N. Linden, H. Barjat, and R. Freeman, *Chem. Phys. Lett.* **296**, 61 (1998).
 [15] D. Collins, K. W. Kim, W. C. Holton, H. Sierzputowska-Gracz, and E. O. Stejskal, *Phys. Rev. A* **62**, 022304 (2000).
 [16] Jaehyun Kim, Jae-Seung Lee, Soonchil Lee, and C. Cheong, *Phys. Rev. A* **62**, 022312 (2000).
 [17] R. Marx, A. F. Fahmy, J. A. Myers, W. Bermel, and S. J. Glaser, *Phys. Rev. A* **62**, 012310 (2000).
 [18] J. A. Jones, M. Mosca and R. H. Hansen, *Nature (London)* **393**, 344 (1998).
 [19] I. L. Chuang, N. Gershenfeld, and M. Kubinec, *Phys. Rev. Lett.* **80**, 3408 (1998).
 [20] J. A. Jones, *Science* **280**, 229 (1998).
 [21] J. A. Jones and M. Mosca, *Phys. Rev. Lett.* **83**, 1050 (1999).
 [22] Lieven M. K. Vandersypen *et al.*, *Appl. Phys. Lett.* **76**, 646 (2000).
 [23] Lieven M. K. Vandersypen *et al.* *Phys. Rev. Lett.* **85**, 5452 (2000).
 [24] S. L. Braunstein, C. Caves, R. Josza, N. Linden, S. Popescu, and R. Shack, *Phys. Rev. Lett.* **83**, 1054 (1999). For a response to this criticism, see R. Laflamme, <http://quickreviews.org/qc/>
 [25] S. Lloyd, *Phys. Rev. A* **61**, 010301(R) (2000).
 [26] J. Ahn, P. H. Bucksbaum, and T. C. Weinacht, *Science* **287**, 463 (2000).
 [27] P. Knight, *Science* **287**, 441 (2000).
 [28] David A. Meyer, *Phys. Rev. Lett.* **85**, 2014 (2000).
 [29] R. Cleve, A. Ekert, C. Macchiavello, and M. Mosca, *Proc. R. Soc. London, Ser. A* **454**, 339 (1998).
 [30] Barbara M. Terhal and John A. Smolin, *Phys. Rev. A* **58**, 1822 (1999).
 [31] J. A. Jones and M. Mosca, *J. Chem. Phys.* **109**, 1648 (1998).
 [32] D. G. Cory, A. F. Fahmy, and T. F. Havel, *Proc. Natl. Acad. Sci. U.S.A.* **94**, 1634 (1997).
 [33] D. G. Cory, A. F. Fahmy, and M. D. Price, *Physica D* **120**, 82 (1998).
 [34] D. W. Leung, e-print at <http://xxx.lanl.gov/abs/quant-ph/004100>; J. A. Jones, e-print at <http://xxx.lanl.gov/abs/quant-ph/9905008>.
 [35] N. Linden, B. Herve, R. J. Carbajo, and R. Freeman, *Chem. Phys. Lett.* **305**, 28 (1999).